ELSEVIER

Energy and Buildings 27 (1998) 137–146

ENERGY AND BUILDINGS

# Natural convective heat transfer rates in rectangular enclosures

R.K. Calay [a,*], A.E. Holdø [a], G.P. Hammond [b]

[a] *Fluid Mechanics Research Group, School of Engineering and Information Sciences, University of Hertfordshire, Hatfield AL10-9AB, England, UK*

[b] *School of Mechanical Engineering, University of Bath, Claverton Down, Bath BA2-7AY, England, UK*

Received 20 April 1997; received in revised form 10 May 1997; accepted 15 May 1997

**Abstract**

An experimental study of buoyancy-driven convection in rectangular enclosures has been made in order to obtain convection coefficients and data correlations which are more accurate for real building situation. Three different flow regimes viz. stably-stratified flow, buoyancy-driven vertical flow and horizontal flow were investigated. The Nusselt number variation with respect to the Rayleigh number has been plotted and compared with existing correlations. In general, the measured data were lower than the data obtained from the existing correlations which are mainly derived from data obtained from experiments involving isolated surfaces. © 1998 Elsevier Science S.A.

*Keywords:* Heat transfer; Convection coefficient; Nusselt number; Rayleigh number

## 1. Introduction

The buoyancy-driven convection plays an important role in the design and performance of naturally-ventilated buildings. Particularly for passive solar buildings the internal energy flows between the thermal mass and inside air are controlled by convective heat transfer coefficients. Their influence on the performance e.g., energy consumption during start up, overheating and thermal comfort can be significant. Many computer based building dynamic thermal model have been developed to be able to design energy-efficient buildings. Unfortunately, the accuracy of these models is presently limited by the uncertainties in the input data, particularly for air infiltration and convective heat transfer rates. The evaluation of convective heat transfer coefficients is still found to be a weak point of these building models. The ideal approach is to solve the conservation equations for the temperature and the velocity fields for a control volume under consideration, which is not practical due to limitations of computing time and capacity. Thus building thermal simulation models employ empirical correlations to calculate convective heat transfer. The majority of the available correlations recommended by the ASHRAE [1] and CIBSE [2] guides are derived from data mainly based on experiments with isolated horizontal and vertical surfaces. Therefore, these correlations may not be accurate when applied to enclosed surfaces with induced airflow as found in buildings.

In the CIBSE guide radiative coefficients are combined with convective coefficients. There is no distinction between forced and natural convection. The following power law correlation with different $n$ for laminar and turbulent flow regimes:

$$\mathrm{Nu} = C\mathrm{Ra}^n \quad (1)$$

leads to a two part correlation. The discontinuity between the two parts causes error in the calculation of the convection coefficients and numerical instability in the models when encountering flows in transition. Alamdari and Hammond [3] derived improved correlations which overcome the instability problem found with the above correlation. Their correlation covers the full range of air flow and varies smoothly between the laminar and turbulent regions. However, their correlation is also based upon the data gathered from experiments using isolated surfaces and thus may not be directly applicable to building applications. A comparative study of the correlations for buoyancy driven convection coefficients based on experimental studies has been presented by Dascalaki et al. [4]. The majority of the reported experimental work used vertical or horizontal flat-plate geometries. There are few studies that used full scale enclosures [5,6]. The convective coefficients based on available correlations vary significantly, thus it is obvious that the variation can influence the energy requirement and thermal analysis results when used in simulation models.

The numerical studies focused mainly on two dimensional flow because of its computational simplicity. Whereas, in

* Corresponding author. Tel.: +44 1707 284124; fax: +44 1707 285086; e-mail: r.k.calay@herts.ac.uk


*PII* S0378-7788(97)00030-3

enclosures with three finite dimensions, the inherent three dimensionality significantly affects the flow pattern and the heat transfer. This implies that numerical studies are more difficult, just where experimental data is scarce. The most critical aspect in the CFD simulations of air flow and heat transfer in buildings is defining the natural convection boundary conditions [7].

The phenomenon of buoyancy-driven steady state convection of a Newtonian fluid in a finite size rigid wall enclosure in a uniform gravitational field exhibits complex boundary conditions. In an enclosure when convection is induced by the temperature difference between the two opposing walls, a boundary-layer will exist near each wall and the central region exterior to the boundary layer will form a central core, which can not be considered independently. This coupling leads to wide variation in flow velocities in the different regions of the enclosure. Raithby and Holland [8] gave much insight into these complexities and arrived a conduction layer model.

The scope of presented investigation is limited to considering an enclosure heated and cooled on opposite sides while remaining sides being adiabatic. Three basic heating regimes occur in the enclosure depending upon the enclosure heated from above, below or from the sides. Each case exhibits different flow regimes for a given set of boundary conditions. Variety of flow structures may occur, in this very simple geometry in the transition from steady laminar to turbulent flows. Thus natural convection in enclosures has been investigated from theoretical aspect such as Rayleigh–Benard problem as well as practical applications such as thermal comfort and solar collectors.

The heat transfer coefficient is a function of temperature difference in two isothermal opposing walls as well as the characteristic length of the surface and the physical properties of the convected fluid. Dimensional analysis may be used to correlate the experimental data showing:

$$h_c = h_c(\beta,\mu,\rho,k,c_p,L,W,\delta,\Delta T,g). \quad (2)$$

Grouping the above parameters into dimensionless form:

$$\mathrm{Nu} = \mathrm{Nu}(\mathrm{Gr},\mathrm{Pr},A_1,A_2). \quad (3)$$

The Nusselt number relation for most fluids may closely be represented by a 'power law' of the form

$$\mathrm{N} = \mathrm{CRa}^n$$

or a correlation of the form

$$\mathrm{N} = \{(\mathrm{ARa}^p)^m + (\mathrm{BRa}^q)^m\}^{1/m}. \quad (4)$$

In vertical enclosures the choice of characteristic length to calculate the Rayleigh number, Ra( $=\mathrm{Gr}\times\mathrm{Pr}$) depends on the type flow regime. In the conduction regime $\delta$ is dominant dimension and in the laminar boundary layer region H is of importance whereas in turbulent region neither is important.

The experimental data obtained in the present study is compared with the most commonly used correlations available in the literature. The purpose of experimental study was to develop a more realistic approach to the understanding of the physical processes of buoyancy-driven convective heat transfer in buildings. It also provides the heat transfer data which more closely represents the real building applications.

## 2. Experimental set-up

The enclosure was one-quarter scale model of a typical room. It was based on 'hot box' arrangement, in which two opposing walls are heated and cooled while others are insulated and act as adiabatic walls (Fig. 1). The hot and cold walls were constructed from 5 mm aluminium plate. The hot wall was heated by a heater mat which consisted of two carbon coated fibre glass mats fixed in between sheet card and held together. One heater mat was used as the main heater to heat the wall while the other acted as the guard heater to prevent the back flow of heat from the main heater. The cold wall was kept at about room temperature by circulating coolant in the cooling jacket. A cooling jacket enclosing a 15 mm diameter coiled copper pipe through which coolant (30% ethylene glycol in water) circulated was welded to the back of the cold plate. A chiller was used to circulate the coolant. Adiabatic wall were constructed from 12 mm thick plywood and painted matt black at inside surface to obtain the emmissivity of the walls nearly equal to the value found in actual rooms. The copper constantan thermocouples (Type T) were

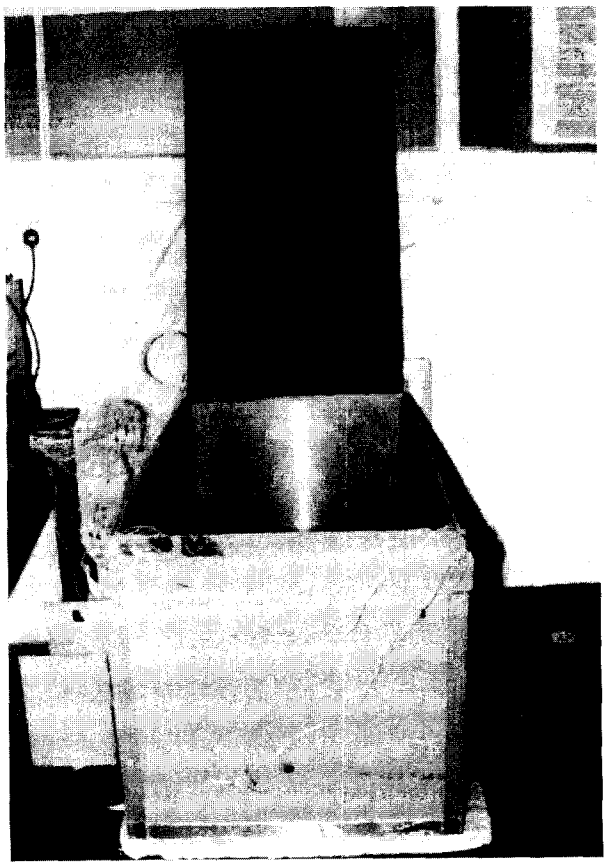

Fig. 1. Experimental rig.

embedded at the surface of each wall to obtain the surface temperature. Thermocouples were also positioned at the outer surface of the adiabatic walls to measure the outer surface temperature in order to include the effect of any heat loss. A wooden frame with thermocouples fixed to it was placed inside the enclosure to obtain the vertical and the horizontal air temperature distribution at the centre of the test cell. The enclosure was insulated with 17 mm fibre insulating board of thermal conductivity (0.06 W/mK) and the whole assembly was fitted into an iron angle frame. Another layer of 50 mm polystyrene sheeting is used to wrap around the whole assembly in order to prevent any heat loss via edges or joints.

Four sets of experiments were performed to simulate the following convective heat-flow configurations:

enclosure heated from side
large vertical walls as hot and cold plates
small vertical walls as hot and cold plates
enclosure heated from below; floor and ceiling as hot and cold plates, respectively
stably stratified convection; ceiling and floor as hot and cold plates, respectively.

For each case the enclosure was assembled in desired orientation. After about 6 or 7 h the power of guard heater was so adjusted to offset any heat loss or heat gain by the main heater. Temperature was recorded once the steady state was reached that usually took about 12 h. A succession of steady state readings was taken for each configuration by varying the heat input to the hot wall over a number of days. The data logging for each case was done overnight after 22:00 to avoid any fluctuations due to lightings, solar gain, people movement in the laboratory. Air temperature inside the laboratory during the data logging period was within $\pm 0.5°$. Detailed description of the experimental procedure can be found elsewhere [9]. Uncertainties in the results were estimated at the 95% confidence level using the method of Kline and McClintock [10].

## 3. Calculation procedure

The thermal state of the boundary of the test-cell was known and assumed to be constant. Boussinesq approximation was assumed to be valid. The conductive heat loss through the adiabatic walls was calculated from the temperature gradient across the walls. The total convective heat flux across the enclosure required in determining the Nusselt number was taken to be equal to the average heat flux at hot and cold wall.

The total heat transferred from the hot to cold wall in the enclosure would consist of radiative and convective components. The total convective heat flux across the enclosure required in determining the Nusselt number was taken to be equal to the average of the heat flux at hot and cold walls i.e.:

$$Q_{av} = \frac{Q_h + Q_c}{2}. \tag{5}$$

The following variables were measured: (a) power supplied to the hot wall which is the total heat transferred at the hot wall, (b) hot and cold wall temperatures to calculate the temperature difference between the hot and cold walls and reference temperature, (c) adiabatic wall temperatures at inner and outer surfaces for determining radiative exchange within the enclosure and conductive heat loss through adiabatic walls.

The total heat flux at the cold wall was determined by subtracting the adiabatic wall losses from the heat input at the hot wall. The net convective heat flux at the hot and cold wall; $Q_h$ and $Q_c$ were calculated by subtracting the corresponding radiative heat flux from each wall total heat flux. Emmisivity of each surface was determined by emissometer. The net radiative heat flux at each surface calculated by a matrix radiosity method using shape factor equations given by ASHRAE [1]. The average heat transfer coefficient is calculated from the average heat flux:

$$h = \frac{Q_{av}}{A\Delta T} \tag{6}$$

and Nusselt number, Nu:

$$\mathrm{Nu} = \frac{h\delta}{k_a}. \tag{7}$$

Eq. (6) can be used to determine local heat transfer coefficient by using local values for heat flux and temperature difference. However for building applications average heat transfer coefficient is more appropriate.

## 4. Results and discussion

Heat transfer coefficients ($h$) for different configurations are computed. The correlations for buoyancy-driven convective heat transfer data are in terms of dimensionless parameters; the Nusselt (Nu) and Prandtl (Pr) and Rayleigh (Ra) numbers or sometimes Grashof (Gr) number is used instead, defined as the ratio of Rayleigh to Prandtl number. The correlations recommended by ASHRAE and CIBSE and other correlations derived from tests with full size enclosures and similar configurations are used for comparing the experimental results. The comparisons are presented in tabular as well as in graphical form. Table 1 listed the correlations used for the comparison. Tables 2–5 compare the experimental data with the data obtained from various correlations. Fig. 2a–d shows the temperature variation inside the enclosure for each configuration.

### 4.1. Enclosure heated from sides

Large walls hot and cold (aspect ratios: $H/\delta = 1$, $L/\delta = 1.824$)
Small walls hot and cold (aspect ratios: $H/\delta = W/\delta = 0.548$)

Heat transfer results were obtained in the range of $3.6 \times 10^8 < \mathrm{Ra} < 1 \times 10^{10}$. The experimental data showed a very

Table 1
Equations employed for comparison

| Equation | Correlation, Nu = | Gr range | Flow condition |
|---|---|---|---|
| *Configuration: vertical side, $T_w$ = constant* | | | |
| CIBSE [2] | $0.48\ Gr^{1/4}$ | $Gr < 10^9$ | laminar |
| ASHRAE [1] | $0.117\ Gr^{1/3}$ | $10^8 < Gr < 10^{12}$ | turbulent |
| Alamdari and Hammond [3] | $[(0.55\ Gr^{1/4})^6 + (0.095\ Gr^{1/3})^6]^{1/6}$ | $10^8 < Gr < 10^{10}$ | turbulent |
| Churchill, Chu [12] | $0.3650.31\ Gr^{1/6}$ | $0 < Gr < \infty$ | laminar/turbulent |
| Khalifa and Marshal [6] | $1.53\ Gr^{0.14}$ | $0.4 \times 10^8 < Gr < 10^{10}$ | |
| *Configuration: horizontal side (floor), $T_w$ = constant* | | | |
| CIBSE [2] | $0.517\ Gr^{1/4}$ | $10^8 < Gr < 10^{10}$ | laminar |
| CIBSE [2] | $0.132\ Gr^{1/3}$ | $10^8 < Gr < 10^{10}$ | turbulent |
| ASHRAE [1] | $0.487\ Gr^{1/4}$ | $10^8 < Gr < 10^{10}$ | laminar |
| Alamdari and Hammond [3] | $[(0.52\ Gr^{1/4})^6 + (0.126\ Gr^{1/3})^6]^{1/6}$ | $0 < Gr < \infty$ | laminar/turbulent |
| Khalifa and Marshal [6] | $1.24\ Gr^{0.24}$ | $5 \times 10^8 < Gr < 10^{10}$ | turbulent |
| *Configuration: stably stratified, $T_w$ = constant* | | | |
| CIBSE [2] | $0.236\ Gr^{1/4}$ | $10^8 < Gr < 10^{10}$ | laminar |
| ASHRAE [1] | $0.218\ Gr^{1/4}$ | $10^8 < Gr < 10^{10}$ | laminar |
| Alamdari and Hammond [3] | $0.56\ Gr^{1/5}$ | $10^8 < Gr < 10^{10}$ | laminar |
| Min et al. [14] | $0.065\ Gr^{0.255}$ | not specified | not specified |

Table 2
Comparison of experimental data with the correlation data

| $Ra \times 10^{-8}$ | $Gr \times 10^{-8}$ | Nu | | | | | |
|---|---|---|---|---|---|---|---|
| | | **Exp** | CIBSE | ASHRAE | Alamdari and Hammond | Churchill and Chu | Khalifa et al. |
| 3.6 | 5.1 | **30.4** | 72.13 | 93.47 | 89.38 | 9.63 | 25.34 |
| 4.5 | 6.37 | **34.5** | 76.27 | 100.69 | 95.18 | 9.96 | 26.14 |
| 5.8 | 8.23 | **35.2** | 81.29 | 109.63 | 102.33 | 10.35 | 27.09 |
| 6.7 | 9.5 | **36.0** | 84.28 | 115.03 | 106.68 | 10.58 | 27.64 |
| 7.5 | 10.6 | **37.1** | 86.69 | 119.44 | 110.1 | 10.76 | 28.08 |
| 8.4 | 11.90 | **38** | 89.21 | 124.1 | 117.07 | 10.96 | 28.54 |
| 9.2 | 13.1 | **38.3** | 91.3 | 127.98 | 132.52 | 11.12 | 28.91 |

Case 1: heated from large side wall, $A_1 = 1$, $A_2 = 1.824$.

Table 3
Comparison of experimental data with the correlation data

| $Ra \times 10^{-9}$ | $Gr \times 10^{-9}$ | Nu | | | | | |
|---|---|---|---|---|---|---|---|
| | | **Exp** | CIBSE | ASHRAE | Alamdari and Hammond | Churchill and Chu | Khalifa et al. |
| 3.1 | 4.39 | **63.6** | 184.86 | 191.59 | 167.67 | 13.41 | 34.25 |
| 3.9 | 5.52 | **64.2** | 210.36 | 206.83 | 179.77 | 13.9 | 35.37 |
| 4.5 | 6.39 | **67.3** | 220.85 | 217.14 | 188.01 | 14.22 | 36.10 |
| 5.0 | 7.1 | **68.6** | 228.74 | 224.9 | 194.19 | 14.46 | 36.63 |
| 5.6 | 7.97 | **69.9** | 237.66 | 233.67 | 201.23 | 14.7 | 37.23 |
| 6.0 | 8.55 | **71.2** | 243.3 | 239.22 | 205.64 | 14.8 | 37.6 |
| 6.5 | 9.26 | **74.5** | 249.88 | 245.68 | 210.78 | 15.7 | 38.02 |

Case 2: heated from small side wall, $A_1 = 1$, $A_2 = 0.584$.

wide variation when compared with various correlations (Tables 2 and 3). The experimental value for Nu number is slightly higher than that yielded from the correlation by Khalifa and Marshall [6] based on full-size test facility. This contradicts the belief that values for Nu obtained from the correlations derived from experiments in small and simplified test enclosures are smaller because the flow is confined for these configurations [11]. Because conditions of a real room can be adequately simulated having a small enclosure geometrical similar and ensuring the equivalence of Rayleigh

Table 4
Comparison of experimental data with the correlation data

| $Ra \times 10^{-8}$ | $Gr \times 10^{-8}$ | Nu | | | | | |
|---|---|---|---|---|---|---|---|
| | | **Exp** | CIBSE (laminar) | CIBSE (turbulent) | ASHRAE | Alamdari and Hammond | Khalifa et al. |
| 4.5 | 6.37 | **30.1** | 82.14 | 113.6 | 77.38 | 111.7 | 160.87 |
| 5.8 | 8.23 | **33.8** | 87.55 | 123.7 | 82.47 | 121.2 | 171.03 |
| 6.6 | 9.36 | **34.5** | | 129.1 | 85.18 | 126.4 | 176.42 |
| 6.8 | 9.66 | **35.5** | 91.14 | 130.5 | 85.85 | 127.7 | 177.74 |
| 8.2 | 11.66 | **36.3** | 95.51 | 138.9 | 89.96 | 135.6 | 185.91 |
| 8.6 | 12.2 | **38.9** | 96.65 | 141.1 | 91.04 | 137.6 | 188.05 |

Case 3: heated from below, $A_1 = 1$, $A_2 = 1.82$.

Table 5
Comparison of experimental data with the correlation data

| $Ra \times 10^{-8}$ | $Gr \times 10^{-8}$ | Nu | | | | |
|---|---|---|---|---|---|---|
| | | **Exp** | CIBSE | ASHRAE | Hammond | Min et al. |
| 3.9 | 5.52 | **7.8** | 38.18 | 33.42 | 31.37 | 11.02 |
| 6.1 | 8.65 | **9.2** | 40.47 | 37.39 | 34.32 | 12.35 |
| 8 | 11.4 | **9.4** | 43.33 | 40.02 | 36.24 | 13.24 |
| 9.14 | 13.0 | **9.6** | 44.81 | 41.39 | 37.23 | 13.7 |
| 10.0 | 14.2 | **10** | 45.83 | 42.33 | 37.91 | 14.02 |
| 11.0 | 15.7 | **10.2** | 46.95 | 43.37 | 38.65 | 14.37 |
| 14.0 | 19.8 | **12.0** | 49.78 | 45.99 | 40.51 | 15.26 |

Case 4: heated from ceiling $A_1 = 1$, $A_2 = 1.824$.

number. Correlations proposed by ASHRAE, CIBSE and Alamdari and Hammond [3] produced higher Nu number values for the same range of Gr number and configuration. This is due to the fact that these correlations are based on the experimental data from the isolated vertical surfaces or enclosures with sufficiently large vertical surfaces, where the flow is unconfined and can be considered two dimensional. On the other hand the correlation of Churchill and Chu [12], which is also based on tests with isolated plate yielded significantly lower Nu number value when compared with the experimental results. It shows the choice of correlation for a certain configuration can lead to overprediction or underprediction of convective rates by upto 30–50%.

In the majority of studies the effect of one aspect ratio, $L/\delta$ is ignored, $L$ being assumed to be very large and the flow can be considered two dimensional. Whereas in the enclosures like the one used in this study heat transfer is influenced by both aspect ratios. Small and similar values of $L/\delta$ and $H/\delta$ lead to increased drag on the side walls thereby inhibiting flow across the enclosure. This leads to measurably reduced rates of heat transfer. The prevailing flow regime in the enclosure also affects the heat transfer. In contrast to the horizontal cavity, for which there is flow only when Ra is greater than a certain critical value, there are convection currents in a vertical cavity for any finite Ra. There is an orderly transition of flow regimes as the Ra increases from 0 to $10^9$. However, Bauman et al. [13] showed that for aspect ratio of 0.5 transition to turbulence is expected for $Ra > 10^{11}$. This implies that the flow in enclosures of realistic aspect ratios would be transitional rather than fully turbulent or laminar. At low values of Ra, horizontal conduction is the dominant process. The end walls merely act to turn the weak gravitational circulation through 180° to form a slowly moving rings in the cavity. This is clear from the temperature profile (Fig. 2a), which shows a small region adjacent to the hot wall, ($Y/H = 1$) where temperature increases rapidly to the average hot wall temperature. Similar situation occurs near $Y/H = 0$, where temperature rapidly decreases to average cold wall temperature. The profile exhibits the substantially linear stable stratification in the core region. However, the flow appears to be non-parallel and is dominated by horizontal intrusions flowing along each of the two adiabatic horizontal walls of the enclosures.

The experimental data was plotted on log–log scale for a range of Rayleigh number against the empirical correlation of Allard et al. based on full scale data [14]. Although the experimental data for large side wall heated ($A_1 = 1$, $A_2 = 1.82$) were obtained for $Gr < 10^9$ and the correlation is applicable for $Gr > 10^9$, a good agreement was found between the correlation data and the experimental data (Fig. 3). In the present study the Nusselt number was calculated for the enclosure based on average convective heat transfer in the enclosure. Whereas in many studies Nusselt number was evaluated based on heat transfer at the heated wall. The exper-

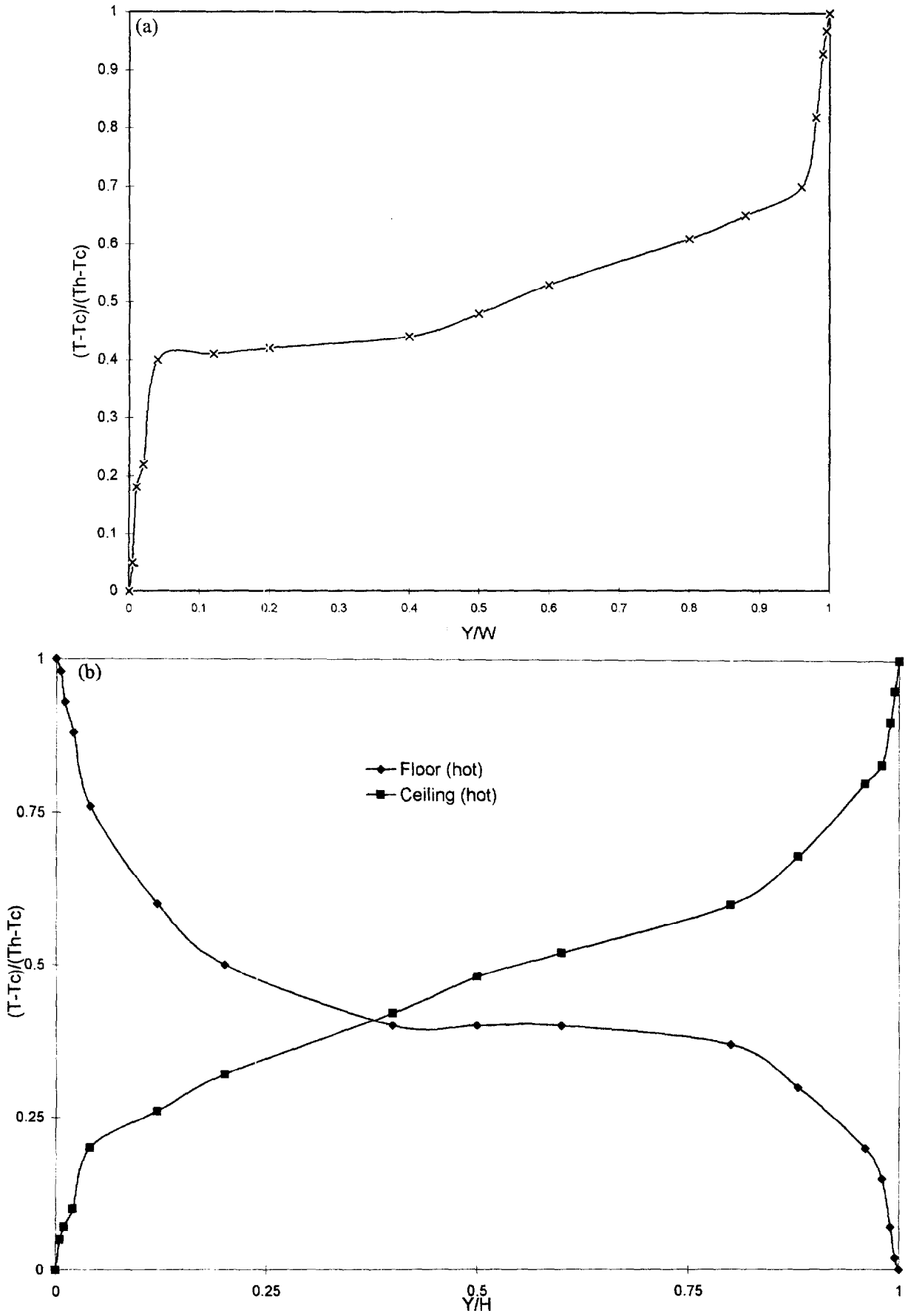


Fig. 2. (a) Horizontal temperature distribution at the mid plane in the cavity. (b) Vertical temperature distribution at the mid plane in the cavity.

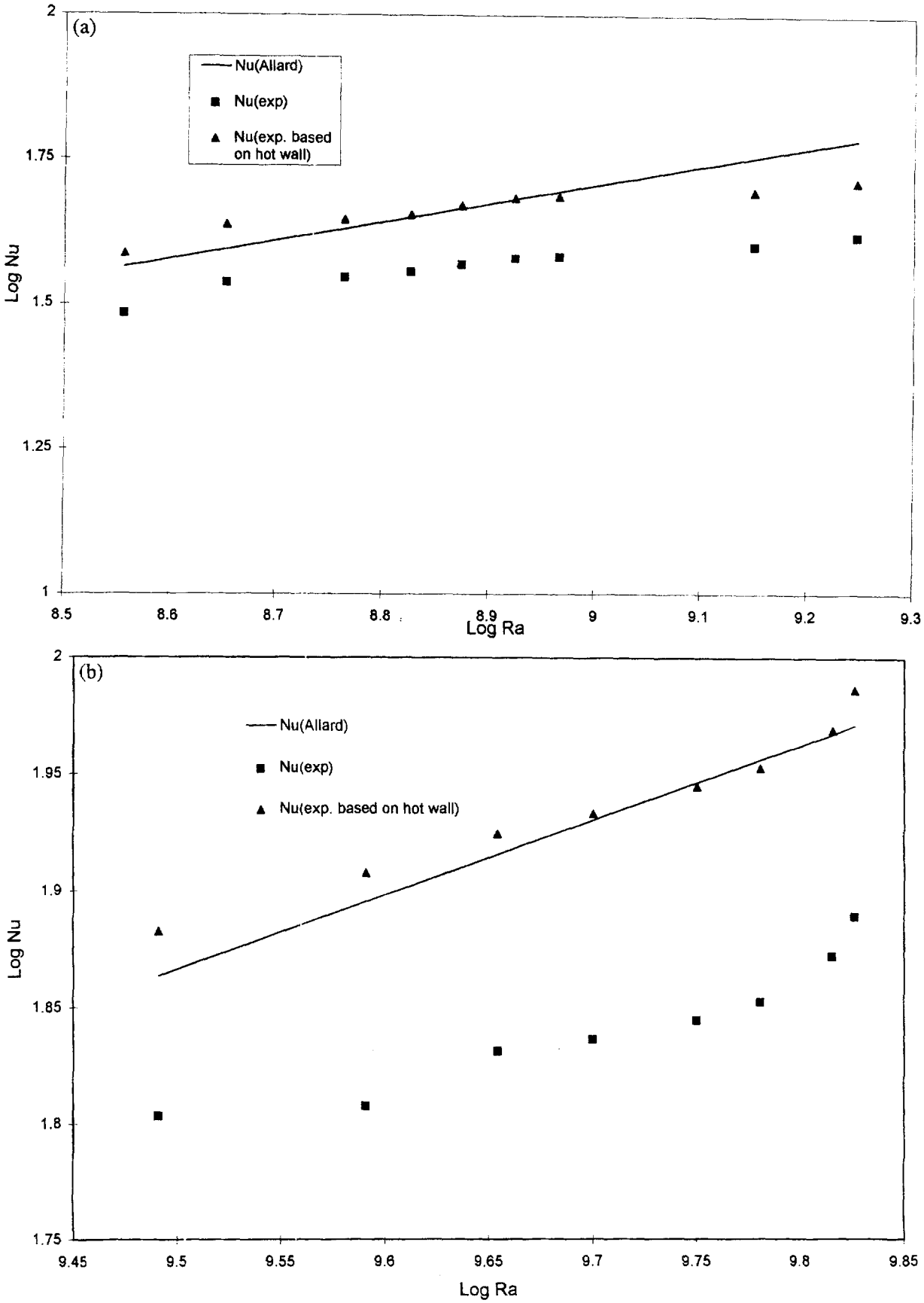


Fig. 3. Comparison of experimental Nu with empirical correlation for a range of Ra number. (a) Large side walls are hot and cold, $A_1 = 1, A_2 = 1.82$. (b) Small side walls are hot and cold, $A_1 = 1, A_2 = 0.584$.

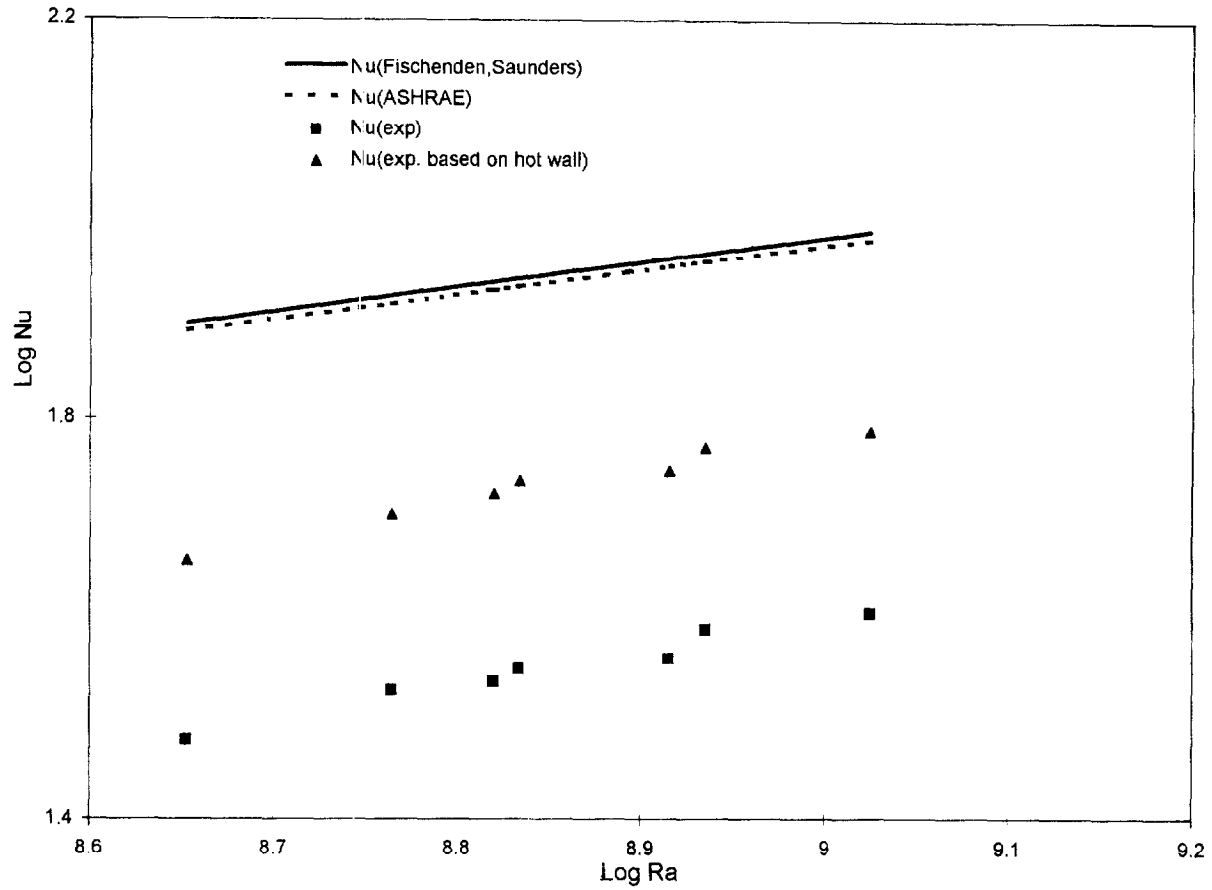


Fig. 4. Comparison of experimental Nu with empirical correlation for a range of Ra number for enclosure heated from below, $A_1 = 1$, $A_2 = 1.82$.

imental Nusselt number when calculated considering heat transfer at the hot wall only showed even better agreement with the full scale data.

### 4.2. Enclosures heated from below

The correlations by CIBSE, ASHRAE, Alamdari and Hammond [3] and Khalifa and Marshall [6] yielded much higher Nusselt number than that obtained from experimental data (Table 4). Strangely the correlation of Khalifa and Marshall which is based on full scale enclosure gave the higher Nu number than the correlations presented in ASHRAE and CIBSE which are based on experimental data mainly for isolated surfaces. When experimental data was based on the heat transfer at the hot wall the agreement was better (Fig. 4).

The experimental and numerical evidence presented in the studies of horizontal cavities reveals that each flow is characterised by a critical Rayleigh number, $Ra_c$, which depends upon the enclosure geometric and thermal properties. There are no exact solution for this critical value. The prediction of $Ra_c$ is very important to any method of correlating Nu–Ra data. At Ra numbers slightly higher than critical Ra, flow consists of steady rolls and the nature of flow becomes increasingly complex with higher Ra numbers which also depends on the Prandtl number. Different values of Ra associated with the onset of turbulence reported in the literature but in general all data suggest that flow is fully turbulent for $Ra > 10^9$.

Temperature profile along the centre line of the enclosure shows rapid change in temperatures near the region close to hot and cold wall.

### 4.3. Enclosures heated from above (stably stratified)

The experimental data were obtained for the range $4 \times 10^8 < Ra < 1.4 \times 10^9$ over which the Nusselt number varied from 7.8 to 11. Again the comparisons with the published correlations provide higher values for Nu number than the experimental values (Fig. 5). This is obvious because CIBSE and ASHRAE correlations are based on data for isolated surfaces. The boundary conditions are completely different for enclosures. The edge effects present in the case of isolated surfaces which are the main driving mechanism of convection are absent in the surfaces bounded by vertical walls. However the correlation by Min et al. [14] which is based on full size enclosures showed better agreement with the experimental results. Nevertheless, the experimental results are much higher than the common presumption that Nu number will effectively be unity over all values of Ra for stably stratified layers in enclosures that is based on the assumption that heat transfer is only possible by in this regime. There is very little experimental evidence to verify this presumption and the

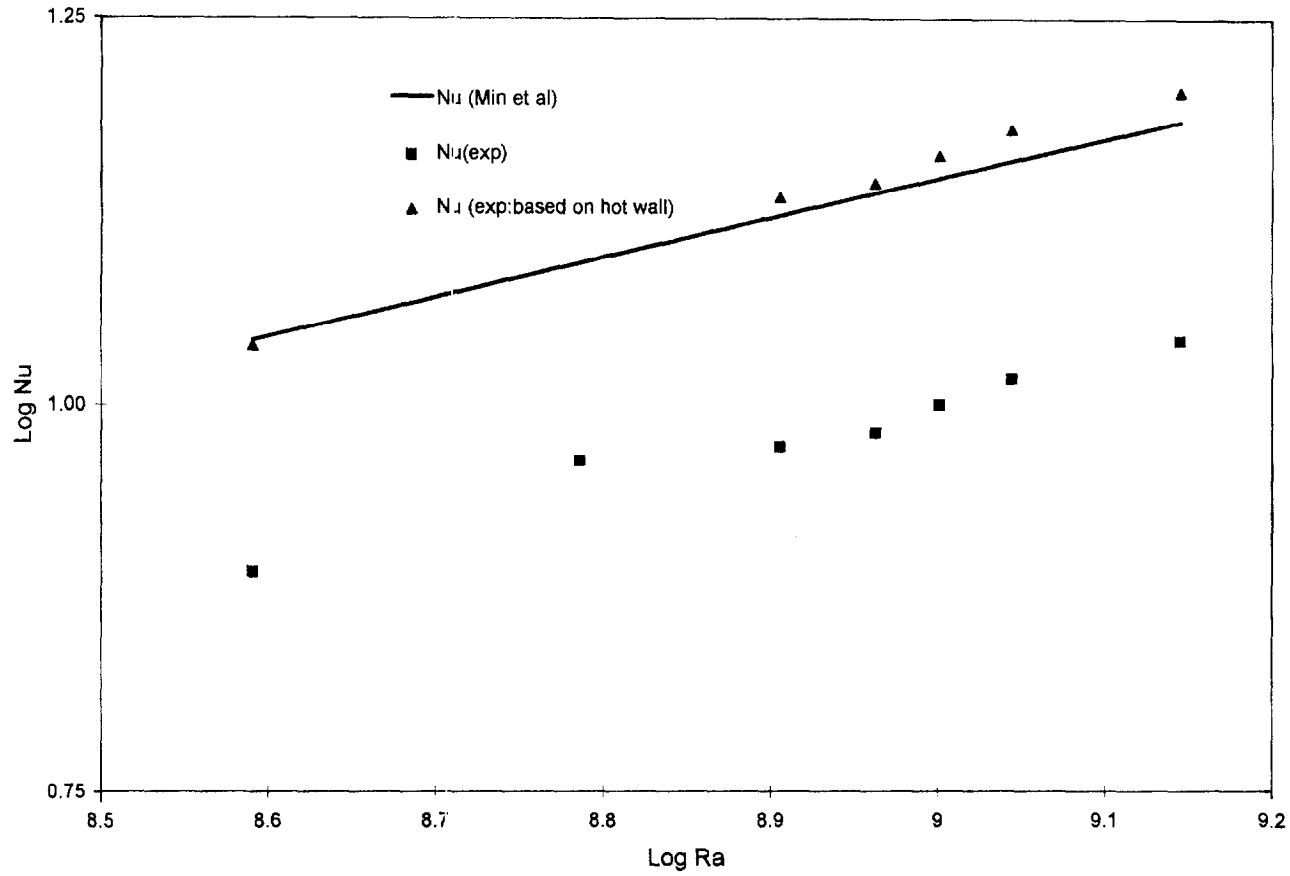


Fig. 5. Comparison of experimental Nu with empirical correlation for a range of Ra number for enclosure heated from above (stably-stratified case), $A_1 = 1$, $A_2 = 1.8$.

experimental data seem to contradict this. The analytical results of Singh et al. [15] based on integral boundary layer equations indicate that Nu in stably stratified layers varies according to a 1/5 power of the Ra number.

The values of heat transfer coefficients for stably-stratified in enclosures can vary by orders of magnitude depending upon the assumptions that are made. The experimental data are very scarce and very different values have been suggested by different researchers.

## 5. Conclusions

In general the correlations proposed by CIBSE and ASHRAE journal yielded much higher Nu number values than the values obtained experimentally. This was expected, because CIBSE and ASHRAE correlations are based on data obtained from experiments for isolated surfaces. Some correlations selected for comparison were based on full scale test data. In some cases the experimental data show good agreement with the data obtained from correlations that are based on similar configuration. Nu number data for vertical wall configuration for aspect ratios 1, 1.824 were found to be in a better agreement than data for aspect ratios 1 and 0.584.

The data for heated horizontal surfaces upward (floor heating) showed a large discrepancy with the data from a full scale experimental study. Natural convection in an enclosure heated from below is very complex problem and has been studied over the past century. The flow structure above, below or at critical Ra is affected by a different set of parameters including geometry of the enclosure and physical characteristics of the fluid. Thus any Nu–Ra correlation is sensitive to the critical Ra for a certain flow configuration. The correlation presented in the literature yield data with very wide variation.

The information for the stably-stratified configuration is even scarcer. However, a good agreement was found between the present data and those reported by Min et al. for this configuration. The Nu number obtained was much higher than unity and demonstrates that this is due to more complex thermal boundary conditions that prevail under this configuration in enclosures.

The choice of internal heat transfer coefficients for real enclosure is a matter of debate. A large number of correlations for estimating the natural convective heat transfer coefficient is available in the literature and the data obtained from these correlations may differ by an order of 10 or more. Although the various correlations are reported to be applicable for a given range of Reynolds and Rayleigh numbers, there are parameters which influence the heat transfer. In many studies the various assumptions which have been made, the flow configuration and the local or average value considered are not reported. For example the effect of aspect ratio is often

ignored. Whereas in enclosures the aspect ratios based on both dimensions and the cavity width has considerable effect on the flow pattern as well as heat transfer within the enclosure. Therefore large differences in experimental configuration make it very difficult to compare data obtained from one correlation with the data from another correlation.

Real buildings may have complex geometry and different operating conditions than experimental set-up. The experimental configuration is idealised, but it is still a better representation of a built environment than is an isolated surface on which most of the currently used correlations are based on. However, the significance of combined effects of more than one heated surfaces in buildings have not yet been evaluated. The careful experimental investigations for temperature profiles could also shed light on the heat transfer mechanism taking place in such enclosures and propose modified physical models to resolve the uncertainties.

## 6. Nomenclature

| | |
|---|---|
| $A$ | surface area, $m^2$ |
| $A_1$ | aspect ratio, $(L\,\delta^{-1})$ |
| $A_2$ | aspect ratio, $(W\,\delta^{-1})$ |
| $c_p$ | specific heat capacity at constant pressure, J $kg^{-1}$ $K^{-1}$ |
| $e$ | emissivity of surface |
| Gr | Grashof number( $=g\beta(T_h-T_c)/\delta^3/\nu^2$) |
| $H$ | enclosure height, m |
| $h_c$ | convective heat transfer coefficient, W $m^{-2}$ K |
| $k_a$ | thermal conductivity of air, W $m^{-1}$ K |
| $L$ | length of enclosure |
| $Nu_\delta$ | surface averaged Nusselt number ( $=h_c\delta k^{-1}$) |
| Pr | Prandtl number, ( $=\mu c_p k^{-1}$) |
| $q$ | heat flux per unit area, W $m^{-2}$ |
| $Q_h$ | heat flux at hot the wall, W |
| $Q_c$ | heat flux at cold wall, W |
| $Q_{av}$ | average heat flux, W |
| Ra | Rayleigh number, ( = Gr Pr) |
| $T_c$ | mean surface temperature of cold wall, °C |
| $T_h$ | mean surface temperature of hot wall, °C |
| $T_f$ | film temperature, ( $=(T_c+T_h)/2$) |
| $W$ | width of the enclosure, m |

*Greek symbols*

| | |
|---|---|
| $\alpha$ | thermal diffusivity, ( $=k/\rho c_p$) |
| $\beta$ | coefficient of thermal cubic expansion, $m^{-3}$ |
| $\delta$ | distance between hot and cold wall, m |
| $\mu$ | viscosity, kg $m^{-1}$ $s^{-1}$ |
| $\nu$ | kinematic viscosity, ( $=\mu/\rho$) |
| $\rho$ | density, kg $m^{-3}$ |

## References


[1] ASHRAE, Fundamental Handbook, ASHRAE, Atlanta, 1985.
[2] CIBSE, CIBSE Guide, Vols. A, B and C, CIBSE, London, 1986.
[3] F. Alamdari, G.P. Hammond, Building Services Res. Technol. 4 (1983) 106–112.
[4] E. Dascalaki, M. Santamouris, C.A. Balaras, D.N. Asimakopoulos, Energy Buildings 20 (1994) 243–249.
[5] F. Allard, J. Brau, C. Inard, J.M. Pallier, Energy Buildings 10 (1987) 49–58.
[6] A.J.N. Khalifa, R.H. Marshall, Int. J. Heat Mass Transfer 33 (1990) 2219–2236.
[7] P.G. Schild, P.O. Tjelflaat, D. Aiulfi, Guidelines for CFD modelling of atria, SINTEF Report No STF11 S95001, N-7034 Trondheim, Norway, Feb. 1995.
[8] G.D. Raithby, K.G.T Hollands, Hand Book of Heat Transfer Fundamentals, 2nd edn., McGraw-Hill, New York, 1985.
[9] R. Kaur, Experimental study of buoyancy-driven convection in air filled rectangular enclosures, MSc. thesis Cranfield Inst. of Technol., Cranfield, UK, 1990.
[10] S.J. Kline, F.A. McClintock, describing uncertainties in single sample experiments, Mechanical Engineering, 3–8 Jan. 1953.
[11] F. Bauman, A. Gadgil, R. Kammerud, E. Altmayer, M. Nansteel, AHRAE Trans. 89 (1985) 215–230.
[12] S.W. Churchill, H. Chu, Int. J. Heat Mass Transfer 18 (1975) 1323–1329.
[13] F. Bauman, A. Gadgil, R. Kammerud, R. Grief, Bouyancy-driven convection in rectangular enclosures: Experimental results and numerical calculations, in: Proceedings of the 19th National Heat Transfer Conference, ASME, Paper 80-HT-66, Orlando, FL, 1980.
[14] T. Min, L. Schutrum, G. Parmelee, J. Vouris, ASHRAE Trans. 62 (1956) 337–358.
[15] S.N. Singh, R.C. Birkebak, R.M. Drake, J. Heat Mass Transfer 2 (1969) 87–98.